

Image Cover Sheet

CLASSIFICATION

UNCLASSIFIED

SYSTEM NUMBER

149796

**TITLE**INFRARED REFLECTANCE AND RESPONSIVITY OF PbBiSrCaCuO FILMS**System Number:****Patron Number:****Requester:****Notes:****DSIS Use only:****Deliver to:** FF

PROCEEDINGS REPRINT

 SPIE—The International Society for Optical Engineering

Reprinted from

Infrared Technology XX

**25–28 July 1994
San Diego, California**



Volume 2269

Infrared reflectance and responsivity of PbBiSrCaCuO films

L. Ngo Phong

Defence Research Establishment Valcartier
P. O. Box 8800, Courcellette, QC G0A 1R0, Canada

I. Shih and P. Laou

McGill University, Department of Electrical Engineering
3480 University Street, Montreal, QC H3A 2A7, CanadaABSTRACT

PbBiSrCaCuO films with a predominant $\text{Bi}_2\text{Sr}_2\text{Ca}_2\text{Cu}_3\text{O}_{10}$ superconducting phase were prepared on (100) MgO and LaAlO₃ substrates. The radiative properties of the film-substrate composites were investigated at room temperature and at temperatures near T_c in the wavelength band of 2-17 μm . For the film parameters used in this experiment, the near normal-incidence values of the reflectance were large while those of the transmittance were very small. No significant change in reflectance was observed as the film underwent a superconducting-normal transition in the vicinity of T_c . However, the reflectance decreased with decreasing film thickness and radiation wavelength. It could be verified that the substrate has a negligible effect on overall radiative properties when film thickness is sufficiently large. To determine the response mode of the film at infrared wavelengths, photoresponses to short laser pulses were measured. From the temperature-dependent behavior of transient structure and responsivity, the thermal origin of the photoresponse could be confirmed.

Keywords: high temperature superconductor, BiSrCaCuO, thin film, infrared, reflectance, photoresponse.

1. INTRODUCTION

The interaction between electromagnetic radiation and superconducting films may lead to different response modes that can be used for radiation detection. Under certain modes the film behaves as a square law detector, that is, the magnitude of the electric signal generated across the film is proportional to the radiation power it absorbs. Therefore, to optimize detector design, it is important to investigate the radiative properties and response modes of superconducting films. Recently, several studies were performed on high T_c YBa₂Cu₃O₇ films. Zhang *et al.*¹ measured the infrared reflectance and transmittance of the film-substrate composites with film thicknesses of 10 to 200 nm. Their data showed that reflectance increases with increasing wavelength and could be as large as 0.7. A similar observation was reported by Phelan *et al.*², who computed the spectral reflectance of superconducting-state films using an approximate form of the Mattis-Bardeen theory. In their study the reflectance computed at infrared wavelengths was larger than 0.85. Further calculations for very thin films also suggested that the film-substrate absorptance decreases when film thickness is increased.³ It is still questionable, however, whether the infrared photoresponse of the film is thermal or nonthermal in origin.^{4, 5} A clear result would provide insight into the appropriate design for

superconducting detectors. For instance, absorptance is a critical parameter for thermal detectors. If photoresponse is thermal and absorptance is too small, antireflective coating may be required for enhancing detector performance in the spectral range of interest.

Few studies have been performed on the $\text{Bi}_2\text{Sr}_2\text{Ca}_2\text{Cu}_3\text{O}_{10}$ films although detectors based on these films can operate at temperatures above 100 K. This may be because it is difficult to obtain a single high T_c phase in these films under normal preparation conditions. We have lately prepared nearly single phase films using lead doping combined with a short heat treatment process.⁶ In considering the use of these films for radiation detection, we have examined their radiative properties. In this paper, the results obtained for relatively thick films (film thickness ~ 200-600 nm) are reported. The near normal-incidence reflectance and transmittance of the film-substrate composites and of the substrates were measured at infrared wavelengths for different temperature ranges. In addition, the responsivity to short laser pulses was investigated in order to determine the photoresponse origin. From the analysis of the results, methods for optimizing the performance of superconducting detectors are discussed.

2. RADIATIVE PROPERTIES

2.1. Film samples

Magnetron rf sputtering was used to deposit PbBiSrCaCuO films onto (100) MgO and LaAlO_3 monocrystalline substrates. The film thickness, in the 200-600 nm range, was monitored from the deposition time and measured with a surface profiler (Sloan Dektak 3030). The thicknesses of the MgO and LaAlO_3 substrates were 310 and 230 μm , respectively. All substrates are one-side polished with film deposited on the polished side. After the deposition, the films were heat-treated successively in flowing oxygen for 20 minutes and in air for 40 minutes. The annealing temperatures in oxygen and in air were 830 and 865 $^\circ\text{C}$, respectively. Whereas the surface of the as-deposited film was smooth, that of the treated films showed a roughness of approximately 30 nm, probably due to a liquid state reaction during the heat treatment. Figure 1a presents the x-ray (1.54 \AA $\text{CuK}\alpha$) diffraction spectrum for a treated film deposited on MgO . This spectrum contains almost uniquely (00 l) Bragg diffraction peaks of the $\text{Bi}_2\text{Sr}_2\text{Ca}_2\text{Cu}_3\text{O}_{10}$ phase, suggesting the film is nearly single phase with a preferred c -axis orientation normal to the substrate surface. To verify this, the ac magnetic susceptibility of the film was measured. Figure 1b shows the temperature dependence of the inductive (χ') and resistive (χ'') components of the complex susceptibility $\chi = \chi' + j\chi''$. We note two main features here. First, the film undergoes a transition from diamagnetic state to normal paramagnetic state near the T_c value of the $\text{Bi}_2\text{Sr}_2\text{Ca}_2\text{Cu}_3\text{O}_{10}$ phase. χ' is seen to change accordingly from its limit of -1 to a small positive value near $T_c \sim 105$ K. χ'' also transforms from the diamagnetic state to the normal state zero through a peak near 105 K. Second, the treated film is mainly single phase as the intergrain coupling appears to be strong. Because χ'' may be related to energy dissipation, the value of χ'' is peaking at the temperature where the resistive losses across the Josephson junctions are maximum. Losses of this type occur when the field-induced current exceeds the Josephson current. Therefore, the intergrain coupling strength may be scaled inversely to the sensitivity of χ'' to magnitude changes of the applied field H . From the results of susceptibility measurement, we noted that the effect of field amplitude is weak for the treated films and is significant for films with a mixed $\text{Bi}_2\text{Sr}_2\text{CaCu}_2\text{O}_8$ / $\text{Bi}_2\text{Sr}_2\text{Ca}_2\text{Cu}_3\text{O}_{10}$ phase. For example, when H was increased from 25 to 800 A/m, the χ'' peak for the treated films shifted by ~ 3 K towards lower temperatures

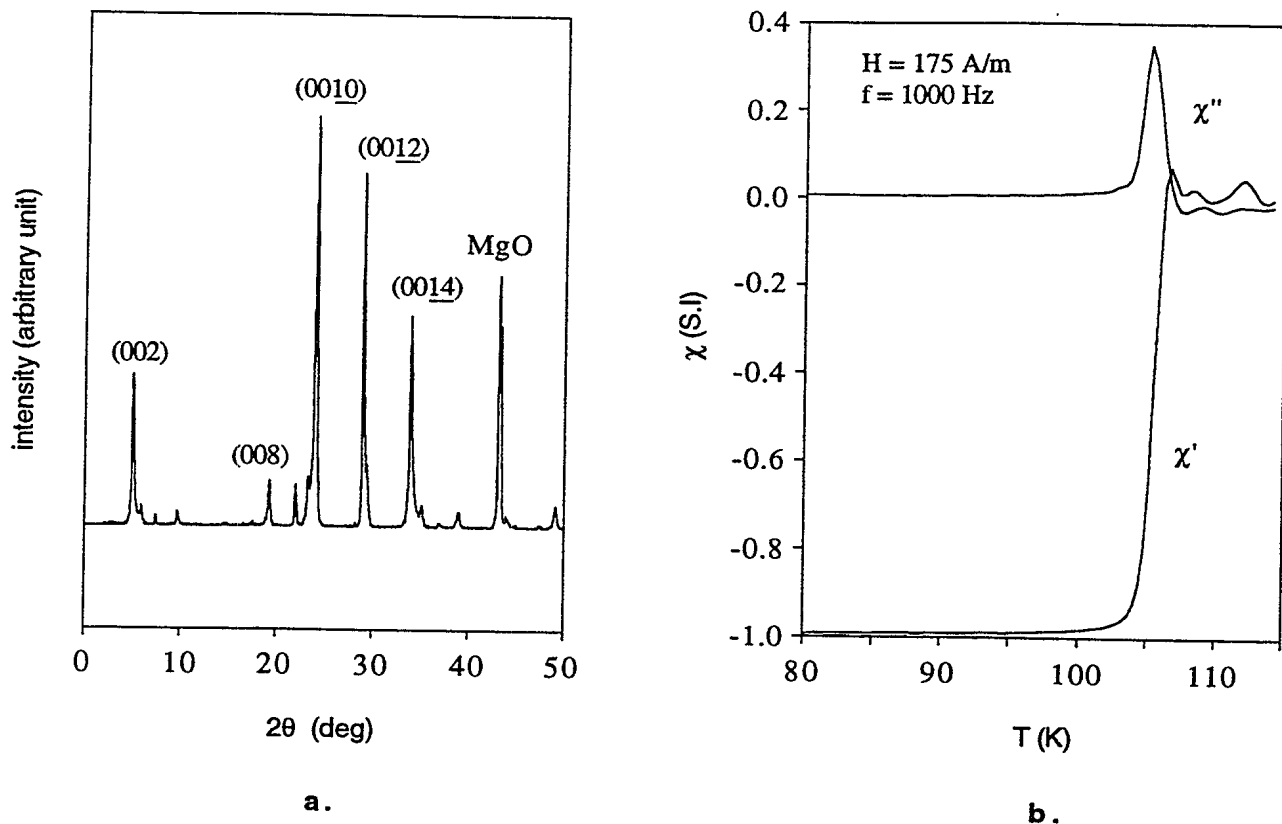


FIG. 1. *a.* XRD spectrum of a treated PbBiSrCaCuO film. The identified Bragg diffraction peaks are the (00 l) peaks of the Bi₂Sr₂Ca₂Cu₃O₁₀ superconducting phase. *b.* Temperature dependence of the ac complex magnetic susceptibility of the same film.

whereas the χ'' peak for a mixed phase film shifted by ~ 16 K.⁷

2.2. Experimental details and results

2.2.1. Room temperature measurement

A Perkin Elmer 297 infrared spectrophotometer was used for the room temperature measurement of the near normal-incidence reflectance (ρ) and normal-incidence transmittance (τ) of the samples. The latter included film-substrate composites and bare substrates. The wavelength range of the spectrophotometer was 2-17 μm . An Au mirror was used as the reference for the reflectance measurement. The reflectance of the Au mirror was evaluated to be 0.99 for all wavelengths.⁸ The ratio of the spectral response with the sample to the spectral response with the mirror was taken as the spectral reflectance of the sample. With the sample withdrawn so that the beam was directly incident on the detector located behind the sample, the transmittance measurement was calibrated by adjusting τ to unity.

Figure 2a shows the spectral reflectance and transmittance of the film-substrate composites for

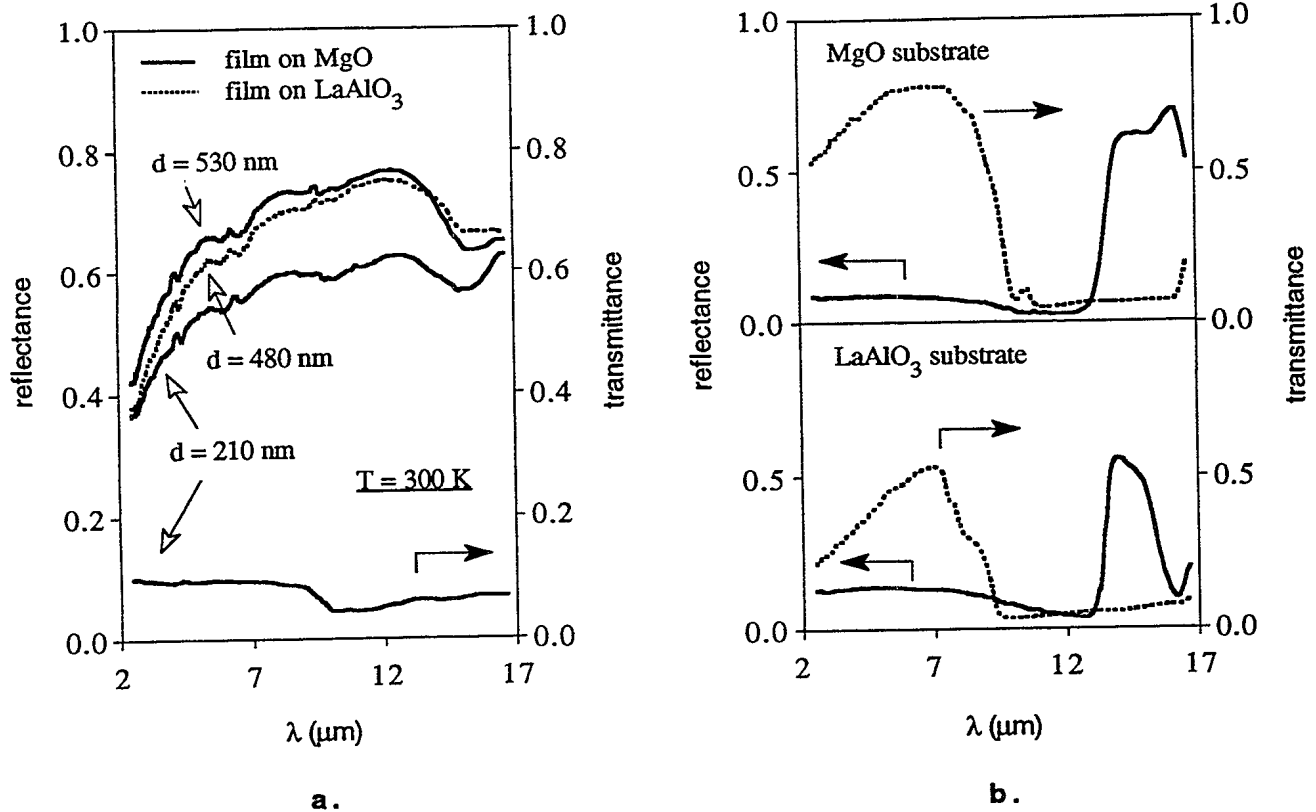


FIG. 2. *a.* Spectral reflectance and transmittance of PbBiSrCaCuO film on MgO or LaAlO₃ substrate, measured at room temperature for different film thicknesses. *b.* Spectral reflectance and transmittance of MgO and LaAlO₃ substrates without film. The substrate thicknesses were 310 and 230 μm , respectively.

different film thicknesses d . Those of the MgO and LaAlO₃ substrates are presented in Fig. 2b. The radiative properties measured for the LaAlO₃ substrate are quite similar to those reported by Zhang *et al.*¹. The small difference in the substrate transmittance may be due to the fact that our substrate (230 nm) is thinner than the one used by the above authors (446 nm) so that it is not totally opaque for $\lambda > 9\ \mu\text{m}$. The spectral behavior of the composite reflectance followed a common pattern regardless of the film thickness. To illustrate this pattern, consider the reflectance of the composite with $d = 210\text{ nm}$. Here, ρ increases by 50% between 2.5 and 6 μm but does not change very much for the longer wavelengths. In effect, as λ is further increased, ρ reaches a maximum of ~ 0.6 near 8 μm and remains around this value before attaining a small minimum in the vicinity of 15 μm . The reflectance of samples with larger film thicknesses is larger but exhibits essentially an analogous spectral dependence. Referring to the data reported in Ref. 1, we also noted a quite similar dependence for the reflectance of YBa₂Cu₃O₇ film in the 2-12 μm wavelength range. The maximum reflectance reported in this range for a YBa₂Cu₃O₇ sample with $d = 200\text{ nm}$ is about 17% higher than that for the Bi₂Sr₂Ca₂Cu₃O₁₀ sample with $d = 210\text{ nm}$.

Some effects of film thickness on the reflectance and transmittance of the film-substrate composite could be confirmed. First, unless the film is transparent in the spectral range considered, the composite transmittance τ should decrease towards zero when d is increased. Conversely, the spectral values of τ are

anticipated to approach those of the bare substrate when d is decreased. The film-substrate composite was examined and was found to be nearly opaque for d larger than about 400 nm. The fact that MgO and LaAlO₃ substrates have a fairly large transmittance level when $\lambda < 9 \mu\text{m}$ suggests that film transmittance may be very small in the 2.5-9 μm range. As d was reduced to 210 nm, some transmittance could be measured, as shown in Fig. 2a. The transmittance value remains at approximately 0.1 for wavelengths up to $\sim 9 \mu\text{m}$. Beyond this wavelength limit, transmittance drops to a lower level. Since d is relatively small, such a decrease in τ is believed to be due to the influence of the substrate whose transmittance also falls sharply to a low level near $\lambda \sim 9 \mu\text{m}$. However, the influence of the substrate on the overall properties of the composite was negligible when d was large. For example, while the radiative properties of the MgO and LaAlO₃ substrates are quite different (Fig. 2b), the spectral reflectances of the thick films ($d \sim 500 \text{ nm}$) deposited on them are almost coincident (Fig. 2a). The small difference between these reflectances may be attributed to the fact that the corresponding film thicknesses are not exactly identical. It should be noted that, as in the case of YBa₂Cu₃O₇ films, the results obtained for Bi₂Sr₂Ca₂Cu₃O₁₀ films also suggest a decrease in reflectance with decreasing film thickness.

2.2.2 Low temperature measurement

The spectral reflectance and transmittance of Bi₂Sr₂Ca₂Cu₃O₁₀ films were further measured in the 85-120 K temperature range. A schematic diagram of the experimental setup for the low temperature measurement is shown in Fig. 3. The film-substrate composite was thermally anchored to the cold head of a liquid nitrogen cryostat with optical access via a ZnSe window. The sample temperature was monitored by a Si sensor imbedded in the cold head and connected to a feedback temperature controller. A spectrophotometer provided monochromatic light in the 2-9.5 μm spectral range. The beam, chopped at a frequency of 80 Hz, was incident on the sample at an angle of about 5° from the normal of the film surface. For the 2-5 μm range, a calibrated InSb photovoltaic detector (Judson Infrared Inc.) was employed to determine the light intensity. A HgCdTe photoconductive detector (Optikon HCT-50) was used to determine the light intensity for the 5-9.5 μm range. A lock-in amplifier, set at the chopping frequency, was used to detect the electric signals generated at the detectors by the reflected or transmitted light beam. The sensitivity of the lock-in amplifier was set at 1 μV . An Au mirror placed on the bottom of the cryostat was used as the reference for the reflectance measurement. To measure the reflectance, the entire cryostat was moved by a distance so that the beam was incident only on the mirror. The reflectance of the sample was determined as the ratio of the intensity of the beam reflected from the sample to that of the beam reflected from the mirror. To minimize measurement errors, care was taken to ensure identical alignments for cases with the Au mirror and with the samples. For the transmittance measurements, the intensity of the beam reflected from the mirror was first measured. After this the cryostat was moved so that the beam was incident on the sample. The beam transmitted through the sample was reflected by the mirror and detected by the same detector. The transmittance of the sample was determined as the ratio of the intensity measured with the sample to that measured solely with the mirror. To enhance the measurement accuracy, a thick opaque paper was installed on the ZnSe window to separate the reflected beam from the transmitted beam. Furthermore, an opaque mask with a low reflectance was mounted on the ZnSe window to confine the incident beam and to eliminate unwanted reflection from window surfaces.

Figure 4a shows the spectral reflectance of superconducting-state samples of two different film

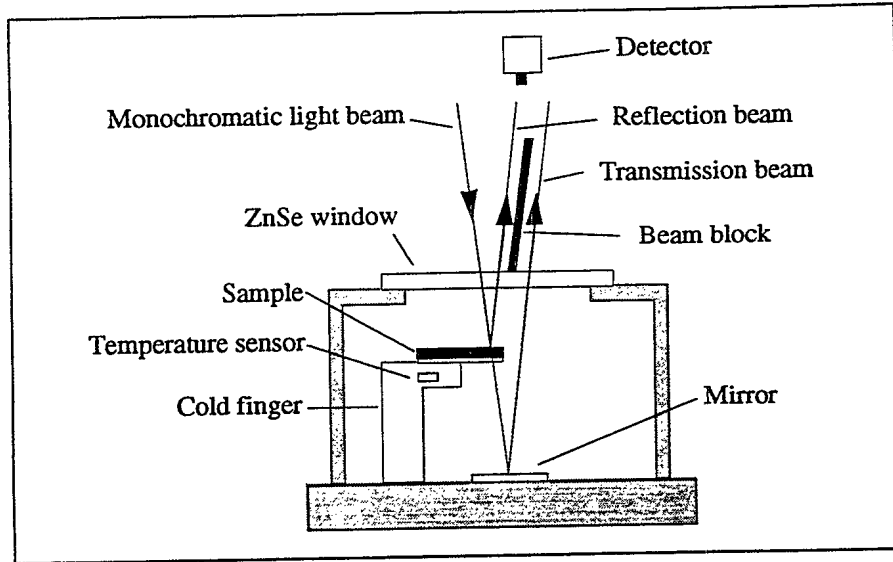


FIG. 3. Schematic diagram of the experimental setup for the low temperature measurement of radiative properties.

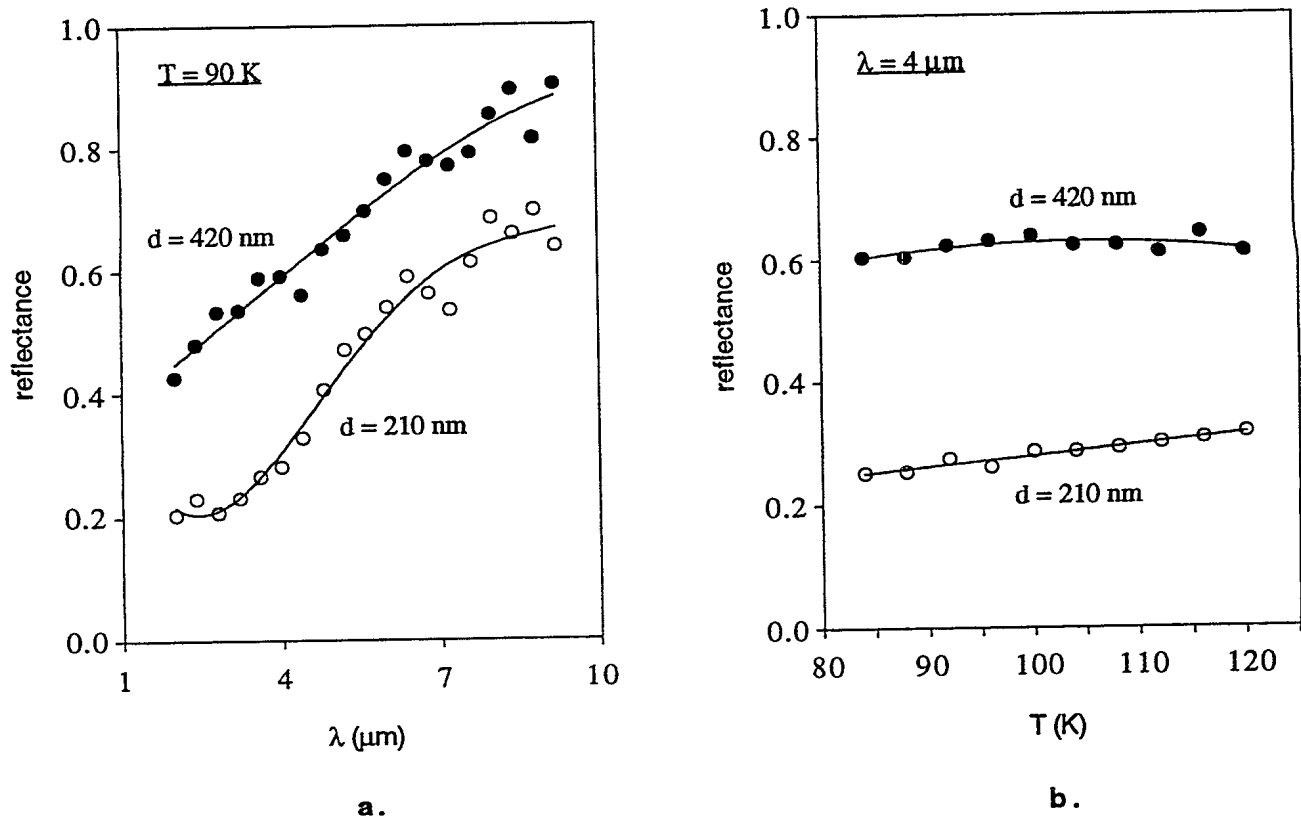


FIG. 4. *a.* Spectral reflectance of PbBiSrCaCuO film on MgO substrate, measured at $T = 90$ K for two different film thicknesses. *b.* Temperature dependence of the reflectance of the above samples, measured at $\lambda = 4$ μm for temperatures in the vicinity of the film resistance transition. Solid lines are provided as visual aids.

thicknesses. First, it can be seen that the reflectance of the sample increases with increasing film thickness and radiation wavelength. This general behavior agrees with the behavior observed at room temperature previously. Second, the values of the reflectance measured at low temperature are comparable to those measured at room temperature. The difference between these values and the 300 K values is less than 36%. Measurement errors and the fact that measurement conditions at room temperature may not be identical to those employed in this experiment account for a major part of this difference. The effect of temperature, therefore, may not be very important. In Fig. 4b, the temperature dependence of the reflectance in the 85-120 K temperature range is shown. No significant change in the reflectance was observed as the film underwent a superconducting-normal transition in the vicinity of T_c .

The transmittance of all the samples was very small and the measured values were in the order of noise level. This is true even for samples with the smallest film thickness ($d = 210$ nm). Therefore, Fig. 4a provides information on the absorptance of the film-substrate composite, estimated as $(1-\rho)$. It should be mentioned that the measured transmittance is smaller than the actual value. A portion of the transmitted beam remains undetected because of light diffusion at the unpolished bottom surface of the substrate. For this reason one should be cognizant that the actual value of the absorptance may be smaller than that appearing in Fig. 4a. This effect is more important at the longer wavelengths where the diffused portion of the transmitted beam is greater. For a 420 nm thick film, absorptance is less than ~ 0.1 at $\lambda = 9.5$ μm . Therefore, antireflective coating, primarily at long wavelengths, would significantly improve the performance of thermal bolometers based on this type of film-substrate structure.

3. INFRARED PHOTORESPONSES

Besides radiative properties, we have investigated the infrared photoresponse of PbBiSrCaCuO films. It was established⁹ previously that interaction between sub-gap photons and superconducting films leads to a thermal and a nonthermal response. A similar result may be expected when the film interacts with above-gap infrared photons. The thermal response is due to radiation heating and hence, occurs for photon energies above and below the superconducting energy gap. On the other hand, nonthermal responses resulting from photodissociation of Cooper pairs¹⁰ and vortex-antivortex pairs¹¹ have been reported. To identify the response mechanism, transient responsivity of PbBiSrCaCuO film to short laser pulses has been measured. The experimental details and results of this study are described in this section.

Some of our films were patterned into meanderline structure with a length-to-width ratio of ~ 40 . Next, Au electrical contacts were formed on the film in four probe configuration by vacuum evaporation. The sample was mounted onto the cold head of a Gifford-McMahon closed cycle cryocooler. An integrated temperature controller provided a temperature stability better than 0.3 mK for the film over an operating range of 10-120 K. The temperature controller was interfaced with a Si sensor imbedded in the cold head and a tightly coupled wire-wound heater. A vibration-isolated system was employed to decouple the film from the vibration induced by the 3 Hz cycling of the cryocooler. Direct optical access to the film was obtained through a KRS-5 infrared window and unwanted radiation from secondary sources was eliminated using a 60 K radiation shield. A low noise current source provided a constant current of up to several tens of mA in the film. The voltage signal generated across the film was driven to a digitizing oscilloscope with a resolution of 500 ps. We are aware that, under certain conditions, the amplitude and transient structure

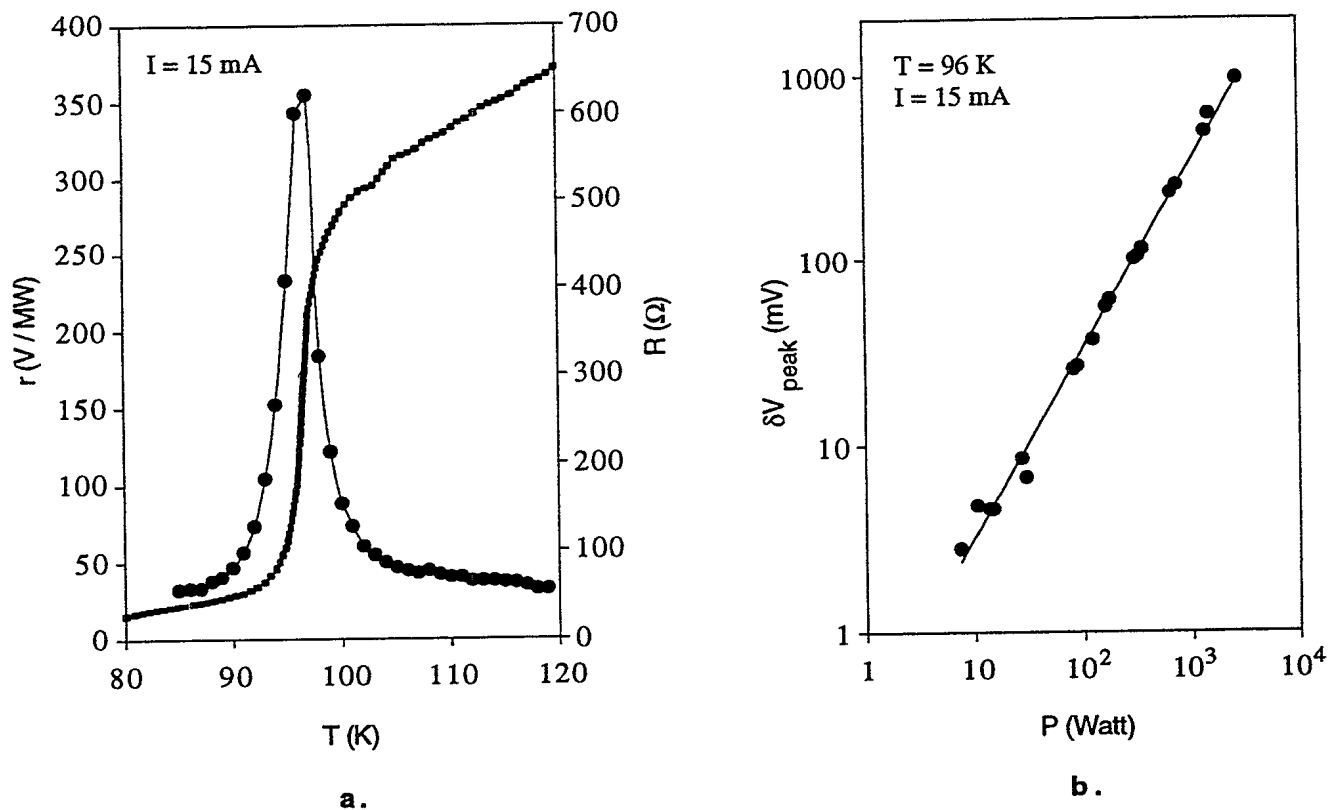


FIG. 5. *a.* Left vertical scale (solid dots): temperature dependence of the film responsivity to Nd:YLF laser pulses for $I = 15$ mA; the solid line is provided as visual aid. Right vertical scale (dashed line): resistance-temperature characteristic of the film measured at $I = 15$ mA. *b.* Peak voltage response to Nd:YLF laser pulses as a function of laser power incident on the film; the solid line depicts a slope of unity.

of the recorded signal may be different from the true characteristics of the generated signal. For example, to avoid mismatch reflection at the oscilloscope and current source, the latter are usually terminated into 50Ω . Such a measuring circuit is appropriate when the bias resistance of the film is much smaller than 50Ω . However, as the film resistance rises the recorded signal amplitude decreases rapidly as a result of the voltage-divider equivalent circuit. This effect may produce important errors as the film resistance can vary significantly when the laser-induced temperature change is large. To prevent these errors, a preamplifier, designed specifically with a high input impedance and a 50Ω output, was inserted between the film and the oscilloscope in the measuring circuit. A transistor circuit was also selected to supply dc current to the film. The high impedance of the transistor collector is desirable to minimize the partial loss of the generated voltage in the current leads of the circuit.

The infrared sources consisted of a Q-switched Nd:YLF laser of $\lambda = 1.05 \mu\text{m}$ and a TEA CO_2 laser with $\lambda = 10.6 \mu\text{m}$. The laser pulses at these wavelengths were characterized, respectively, with an InGaAs photoconductive detector (Newport 818-BB) and a Ge photon drag detector (Rofin 7441). Figure 5a illustrates the temperature dependence of the responsivity r and resistance R of a meanderline film with an active area $S = 7 \text{ mm}^2$. We noted that chemical patterning usually results in some degradation of the super-

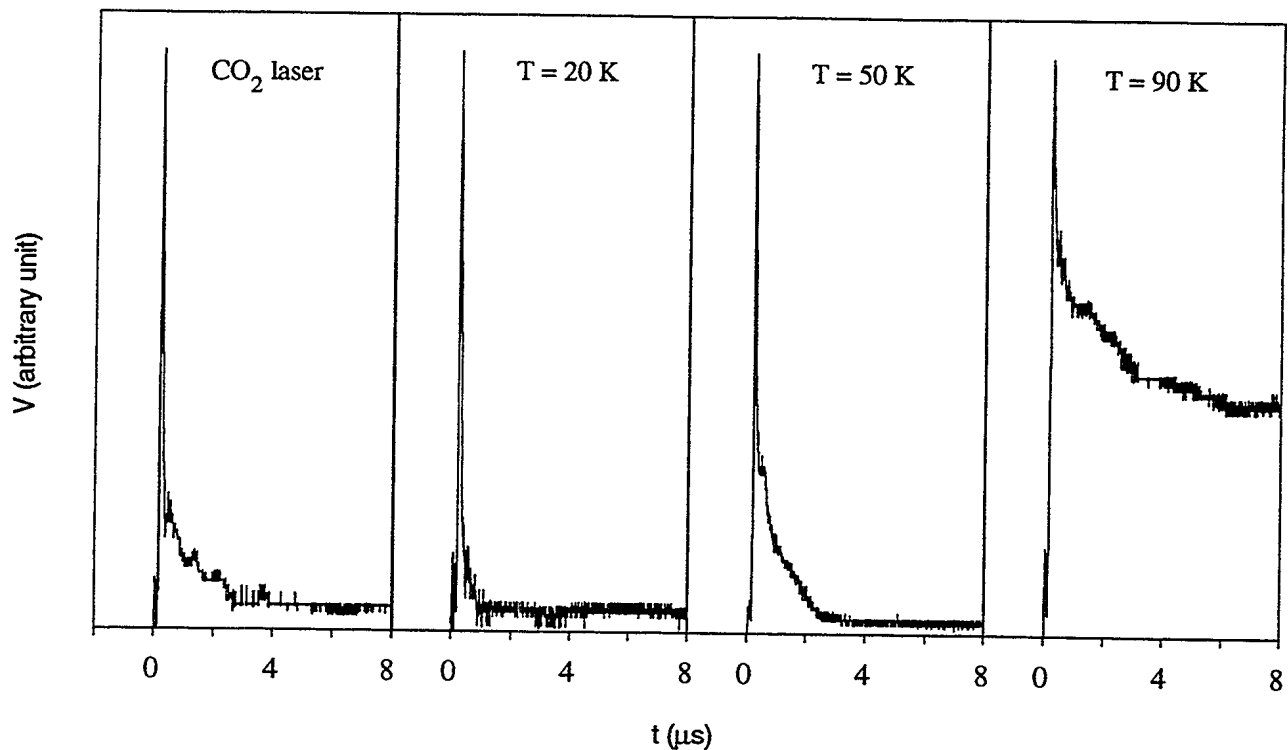


FIG. 6. Effect of bias temperature on the transient structure of the film response to CO₂ laser pulses. The peak voltage of the response is normalized such that it is equal to that of the incident laser pulse.

conductivity of the film. In this example, the resistance transition of the film after the patterning was shifted towards lower temperatures by ~ 7 K. However, the large bias current density ($J \sim 2 \times 10^4$ A/cm²) was mainly responsible for the rather gradual decrease of the resistance to zero. For the responsivity measurement, 3 ns Nd:YLF laser pulses were used to irradiate the film. The peak power density p of the laser incident on the film was approximately 1.75 kW/cm². The temperature dependence of the measured responsivity is indicative of a thermal response. In effect, if the laser-induced temperature rise δT in the film is small, the thermal responsivity can be estimated from $r \approx I (\partial R / \partial T) \delta T / \alpha p S$, where I is the bias current and α is the film absorptance. By assuming a maximum value of $\alpha \sim 0.8$ for the 210-nm thick film (Fig. 4a), good agreement with the measured responsivity was obtained for $\delta T \sim 26$ mK. In further support of thermal origin of the response is the linear power dependence of the peak response in the resistance transition region (Fig. 5b). Such a result could be anticipated from the linear increase of δT with supplied heat energy.

In order to verify whether a nonthermal mechanism occurs at temperatures below T_c , the photo-response of the film in the 20-90 K range was further investigated. For low power densities of the incident laser pulse (i.e. a few kW/cm²), no sign of a nonthermal response was observed. When the power density was increased, the features observed in the recorded transient response suggest that the mechanism is predominantly thermal. The effect of temperature on the transient structure of the response is illustrated in Fig. 6. The peak voltage of the response was normalized so that it is equal to that of the laser pulse for comparison purposes. In this experiment, 85 ns CO₂ laser pulses with $p \sim 260$ kW/cm² were allowed to incident

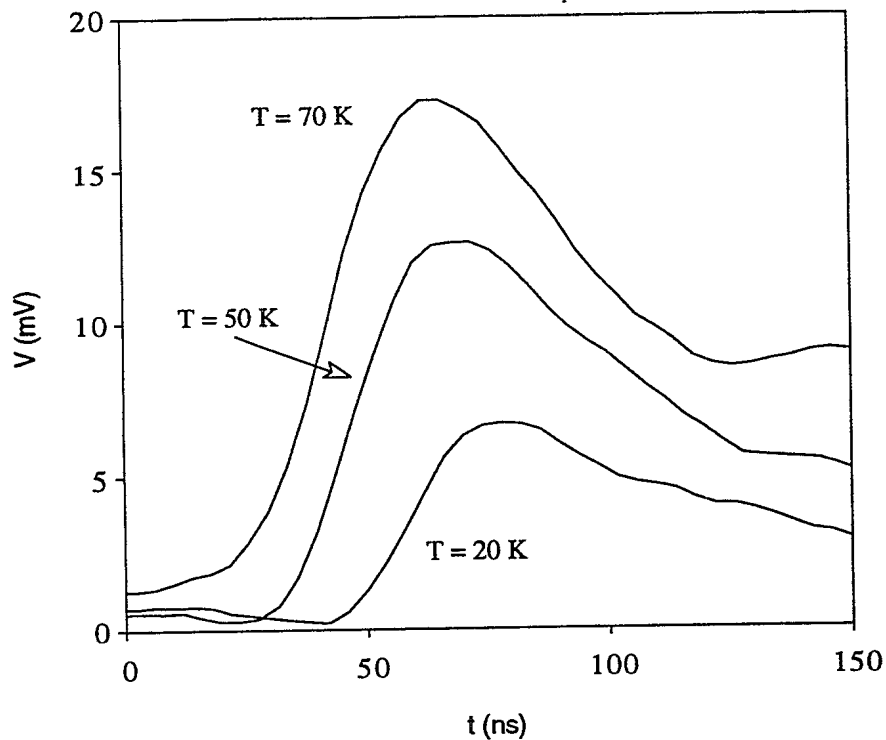


FIG. 7. Effect of bias temperature on the phase shift between the incident and detected signals.

on a film biased at $I = 1$ mA. For the same bias current, the $R - T$ characteristics of the film showed a T_c (onset) of ~ 110 K and a T_c of ~ 90 K. At $T = 20$ K, transient response is seen to decay faster than the incident laser signal. This possibly implies that the response time of the film was shorter than that of the detector used for recording the laser signal, which suggests in turn a nonthermal action. However, this possibility was excluded because the time constant of the Ge photon drag detector (< 1 ns) was much smaller than that of the recorded laser signal. On the other hand, the fast decay observed may be explained qualitatively by the thermal effect. Since the film was biased at a temperature well below T_c , the film responded only after an illumination period during which the delivered heat energy caused the film temperature to rise to about T_c . Conversely, film response ceased after the laser signal had decayed below a threshold level, when the cooling rate became more important than the heating rate. Therefore, the response may only be a reproduction of the top transient structure of the laser signal, which would explain the faster decay. When the bias temperature was increased towards T_c , the decay time of the response also increased. At $T \approx T_c$, the decay time became much larger than that of the incident pulse. These observations, again, imply that the origin of the observed responses was predominantly thermal. The transient responses at different bias temperatures below T_c are plotted on a smaller time scale in Fig. 7. We noted that, when bias temperature was decreased, phase shift between the incident and the detected signals, both of which simultaneously recorded, increased. The occurrence of a phase shift and its temperature dependence support the thermal origin hypothesis. The time delay between the incident and detected signals corresponded with the heating period required to increase film temperature to $\sim T_c$ where a response can be induced. Hence, such a time delay should increase as the temperature difference between T_c and T increases. Another feature

supporting the thermal origin hypothesis is the increase of the peak voltage response with increasing bias temperature (Fig. 7). Assuming that the thermal conductivity and specific heat of the film do not change significantly within narrow temperature ranges below T_c , the laser-induced temperature rise in the film should remain about the same regardless of bias temperatures. Therefore, the maximum value of film resistance attainable by laser illumination is larger when the film is biased at a temperature closer to T_c , which explains the observed increase in peak voltage response.

The results obtained for the conditions used in this experiment confirmed that the infrared photoresponse is predominantly thermal. The absence of the nonthermal response may be attributed to different causes. One possible cause is the relatively large thickness (~ 210 nm) of the film. In a thick film, the recombination time of the quasiparticles is much shorter than the diffusion time. Therefore, the nonthermal signal induced within the absorption depth may be short-circuited by the superconductivity of the dark portion of the film.⁵

4. CONCLUSION

The infrared radiative properties and photoresponses of PbBiSrCaCuO films with a predominant $\text{Bi}_2\text{Sr}_2\text{Ca}_2\text{Cu}_3\text{O}_{10}$ phase were investigated at room temperature and at temperatures near T_c . The near normal-incidence reflectance of samples with film thicknesses of 200-600 nm was large while the near normal-incidence transmittance of the same samples was very small. The effect of temperature on reflectance was not very important. No significant change in reflectance was observed as the film underwent a superconducting-normal transition in the vicinity of T_c . However, the reflectance decreased with decreasing film thickness and radiation wavelength. It could be verified that the substrate has a negligible effect on overall radiative properties when film thickness is sufficiently large. To determine the response mode of the film at infrared wavelengths, photoresponses to short laser pulses were measured at temperatures near and well below T_c . From the temperature-dependent behavior of transient structure and responsivity, the thermal origin of the photoresponse could be confirmed. Because of the thermal origin, the absorptance of infrared detectors which make use of PbBiSrCaCuO films will need to be enhanced. As for future work, the use of antireflective coating, primarily at long wavelengths, will be considered. Furthermore, radiative properties of very thin films will be assessed. If the reflectance can decrease faster than the inverse of transmittance with decreasing film thickness, the absorptance may be anticipated to reach a maximum at some optimum value of film thickness.

5. ACKNOWLEDGMENTS

We are grateful to P. Mathieu for his assistance with the photometric measurements. We also wish to thank B. Tremblay and C. Alain for their technical support.

6. REFERENCES

1. Z. M. Zhang, B. I. Choi, T. A. Le, M. I. Flik, M. P. Siegal, and J. M. Phillips, "Infrared refractive index of thin $\text{YBa}_2\text{Cu}_3\text{O}_7$ superconducting films," *ASME J. Heat Transfer*, Vol. 114, pp. 644-652, 1992.

2. P. E. Phelan, M. I. Flik, and C. L. Tien, "Radiative properties of superconducting Y-Ba-Cu-O thin films," *ASME J. Heat Transfer*, Vol. 113, pp. 487-493, 1991.
3. P. E. Phelan, G. Chen, and C. L. Tien, "Thickness-dependent radiative properties of Y-Ba-Cu-O thin films," *ASME J. Heat Transfer*, Vol. 114, pp. 227-233, 1992.
4. M. G. Forrester, M. Gottlieb, J. R. Gavaler, and A. I. Braginski, "Optical response of epitaxial films of $\text{YBa}_2\text{Cu}_3\text{O}_{7-\delta}$," *Appl. Phys. Lett.*, Vol. 53, pp. 1332-1334, 1988.
5. H. S. Kwok, J. P. Zheng, Q. Y. Ying, and R. Rao, "Nonthermal optical response of Y-Ba-Cu-O thin films," *Appl. Phys. Lett.*, Vol. 54, pp. 2473-2475, 1989.
6. L. Ngo Phong, B. Tremblay, I. Shih, and C. X. Qiu, "Accelerated formation of the high- T_c phase in moderately Pb doped BiSrCaCuO thin films," *Supercond. Sci. Technol.*, Vol. 5, pp. 555-560, 1992.
7. L. Ngo Phong and B. Tremblay, "Superconducting structures and properties of (Pb)BiSrCaCuO films developed under a short annealing," *DREV Report*, 1994 (to be published).
8. W. M. Toscano and E. G. Cravalho, "Thermal radiation properties of the noble metals at cryogenic temperatures," *ASME J. Heat Transfer*, Vol. 98, pp. 438-445, 1976.
9. L. Ngo Phong and I. Shih, "Photoresponses of granular (Pb)BiSrCaCuO films to millimeter wavelength radiation," *J. Appl. Phys.*, Vol. 74, pp. 7414-7421, 1993.
10. Y. Enomoto and T. Murakami, "Optical detector using superconducting $\text{BaPb}_{0.7}\text{Bi}_{0.3}\text{O}_3$ thin films," *J. Appl. Phys.*, Vol. 59, pp. 3807-3814, 1986.
11. J. C. Culbertson, U. Strom, S. A. Wolf, P. Skeath, E. J. West, and W. K. Burns, "Nonlinear optical response of granular Y-Ba-Cu-O films," *Phys. Rev. B*, Vol. 39, pp. 12359-12362, 1989.

#149796

NO. OF COPIES NOMBRE DE COPIES	COPY NO. COPIE N°	INFORMATION SCIENTIST'S INITIALS INITIALES DE L'AGENT D'INFORMATION SCIENTIFIQUE
	1	DAR
AQUISITION ROUTE FOURNI PAR	DREU	
DATE	09 Feb 95	
DSIS ACCESSION NO. NUMÉRO DSIS		

DND 1158 (6-87)



**PLEASE RETURN THIS DOCUMENT
TO THE FOLLOWING ADDRESS:**

DIRECTOR
SCIENTIFIC INFORMATION SERVICES
NATIONAL DEFENCE
HEADQUARTERS
OTTAWA, ONT. - CANADA K1A 0K2

**PRIÈRE DE RETOURNER CE DOCUMENT
À L'ADRESSE SUIVANTE:**

DIRECTEUR
SERVICES D'INFORMATION SCIENTIFIQUES
QUARTIER GÉNÉRAL
DE LA DÉFENSE NATIONALE
OTTAWA, ONT. - CANADA K1A 0K2